

AN ADVANCED ROTATING T-R MAPPING & ITS DIAGNOSES OF TESLA 9-CELL SUPERCONDUCTING CAVITY

Q. S. Shu, G. Deppe, W-D. Moeller, M. Pekeler, D. Proch, D. Renken

P. Stein, C. Stolzenburg, DESY, Hamburg 22603, Germany

T. Junquera, A. Caruette, M. Fouaidy, IPN (CNRS - IN2P3) Orsay, France

Abstract

An advanced rotating temperature and radiation mapping has been developed for investigation of field emission & thermal breakdown of TESLA 9-cell superconducting cavities in superfluid He. More than 10,000 spots on cavity surfaces can be investigated in one turn with 5° angular stepping. We locate a heated area with maximum $\Delta T=3.3\text{K}$ around the 5th cell's equator. A heat flux density of 5 W/cm² in the region $\Delta T=3\text{K}$ and total heat power Q~100W going to LHe from the area were calculated. An emitter responsible for the heating was identified at the iris area ($S_0=8\text{cm}^2$) of the same cell according to T-maps associated with a simulation of impacting electron trajectories. The cavity reached $E_{acc}=20\text{ MV/m}$. We briefly introduce the technical layout, experimental data and analysis results. The surface scanning thermometers, mechanical structure, moving adapting device and a fast data acquisition are discussed in detail in [1], [2].

I. INTRODUCTION

A. Field Emission and Thermal Breakdown

Great progresses have been achieved in pursuing high accelerating gradients of superconducting cavities due to the world-wide efforts [3]. However, the field emission (FE) and thermal breakdown (TB) are still the main obstacles preventing SRF cavities from confidently reaching $E_{acc} = 25\text{ MV/m}$, the TESLA's goal (TESLA is an international effort for the TeV Energy Superconducting Linear Accelerator).

B. T-R Mapping

Most of the FE sources and TB defects on the inner RF surfaces of cavities are submicro-sizes [4] and activated only at high RF fields while cavities in a superconducting state. The main approaches to understand the FE and TB are to study the hot spots and radiation (X-rays induced by impacting FE electrons) on the cavity surfaces during RF operation. Various advanced T and/or R mapping have been developed and comprehensively used at CERN[5], Cornell [6], DESY, Saclay [7] and Wuppertal [8]. T-R mappings can be classified into two categories:

(1) Fixed Mapping: Thermometers (and/or photodiodes) are fixed on the surfaces of cavity. They have higher thermometer efficiency (using grease as bounding agent) in HeII and simpler mechanical structures than rotating one. However, some 700 of thermometers are needed for an one-cell 1.5 GHz cavity [6].

(2) Rotating Mapping: For a 9-cell 1.3 GHz cavity, a rotating T-R mapping uses about 100-150 of thermometers instead of ~ 6,000 (9x700). The thermometer efficiency,

accuracy and reproducibility are highly depending on the heat transfer condition at the sensor location on the cavity wall

The rotating mapping recently developed at DESY combines measurements of T & R for TESLA 9-cell cavities (a complicated geometric structure). Therefore, rather sophisticated mechanical design and surface scanning thermometers is needed to meet all the performance requirements in superfluid He.

II. TECHNICAL LAYOUT

Total 116 specially developed surface scanning thermometers [2] and 32 photodiodes (PIN Silicon/S 1223-01) are assembled into 9-rotating arms as shown in Figure 1 A, B. The thermometer enhance the thermal contact with cavity by a silver tip while isolated from HII with an epoxy housing. Due to a reinforced structure of TESLA cavity, the thermometers can not directly touch the surfaces of cavity iris. Considering the electrical fields reach maximum at iris, 4 photodiodes are mounted in the end of each arm to monitor FE induced X-rays while 14 thermometers are used to monitor the temperatures in the entire region between irises of each cell. Only 9 thermometers are at the first and last arms.

A driving and suspending structure in superfluid He is

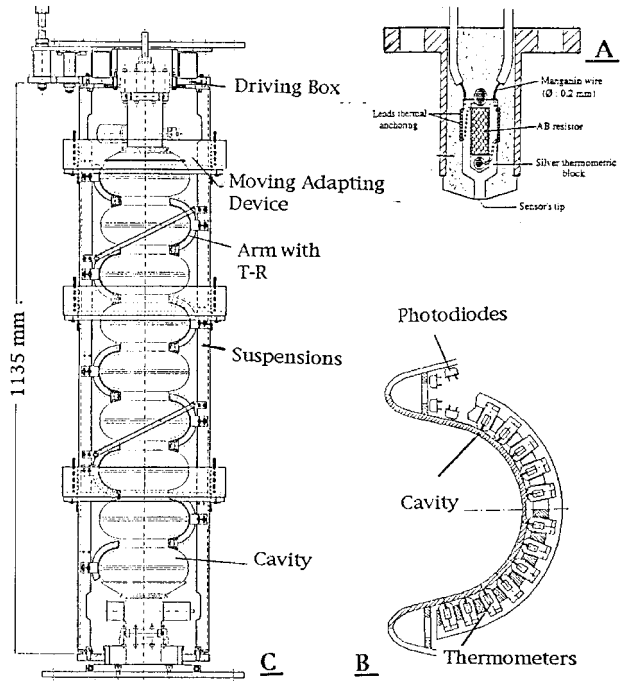


Figure 1: (A) A superfluid He scanning thermometer. (B) A rotating arm. (C) The DESY rotating T-R mapping without rotating measuring cables.

designed to gently turn the arms around and uniformly press the thermometers (through a spring-holder structure, $P=100\text{ g}$

per thermometer) onto the cavity surfaces. A large number of electronic measuring cables have to move with the rotating arms when the T-R mapping rotates. These cable become very rigid in LHe. A moving adapting device is successfully designed to overcome the problem. The space in the TTF vertical cryostat is very constrained that makes the mapping design even more difficult.

Driven by a computer-controlled stepping motor, the T-R arms can be automatically turned to any expected position on the cavity with a accuracy of 1 degree. More than 10,000 spots on cavity surfaces can be investigated in one turn with 5° angular stepping. Two Ge-thermometer and three additional scanning thermometers are used to monitor the change of bath temperature during measurement. Maps can be taken with auto-scanning of entire cavity surface or scanning with time in a fixed position. The effective resolution of temperature measurement is less than 5 mK. One longitudinal measurement in a fixed angular position can be completed in less than 10 ms. All data taken, control and display are performed by a Sun-station computer with a LabView™ language program. Figure 1 C shows the assembly of TESLA T-R mapping without cabling system. The technical aspects will be presented in detail at [1].

III. TEST AND DIAGNOSES

A TESLA prototype cavity -1 has reached 20 MV/m as shown in figure 2. Previously, cavity -1 had been limited by thermal breakdown at about $E_{acc} = 10$ MV/m. Afterwards, the cavity -1 was heat treated at 1400° C in a vacuum oven [9] for one hour with Titanium purification. The cavity was removed 80 µm of material from the inner RF surface and 30 µm from outer side by chemistry, followed by high pressure rinsing with ultra-pure water [9]. Then, the cavity was equipped with the rotating T-R mapping and tested in a vertical cryostat of $T < 2.1$ K.

A. Locating of Heated Areas and Intensity

We successfully locate the heated areas and their intensities associated with processing of cavity RF test. In the test the cavity -1 was initially stopped by heavy field emission at point A of 11.2 MV/m with a $Q, 8.5 \times 10^8$. The T-map

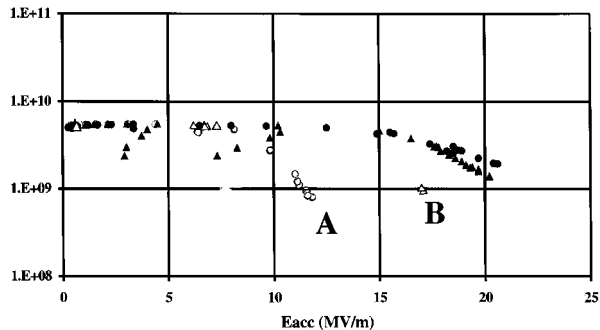


Figure 2: Overall RF performance of the TESLA cavity -1. Dots present first test, triangles present second test. (notice: the low power Q was corrected to about 1×10^{10} by later data)

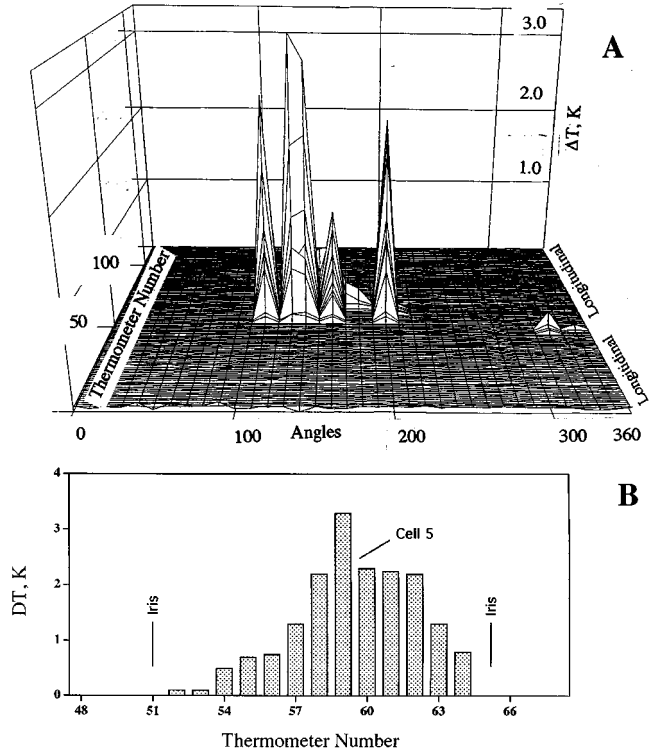


Figure 3: A, A temperature map taken at 11.2 MV/m for TESLA cavity -1. B., Longitudinal ΔT plots, fixed at 140°.

(Figure 3A-3B) indicate an important heated region delimited by 12 thermometers (#53 to #64) centred close to the equator of the 5th cell, between the 110° to 200° angles. out of this region the heating is very low. The ΔT value in this region is 100mK - 3.3K. The x-axial of figure 3 is the thermometer number from 0, close to the top iris of cell-1, to 116, close to the bottom iris of cell-9. The y-axial represents the angular location on the cavity surface. The high pulse RF power processing (HPP, up to $E_{acc}=30$ MV/m) [10] was introduced to the cavity and successfully eliminated the field emitters. Another T-map also witnessed the FE elimination. The shape of Q vs. E plots, map after HPP and FE electron tranjectories indicate that a serious defect heating in the area is excluded. After HPP, the cavity finally reached 20 MV/m in cw mode.

The cavity was stayed in the cryostat and naturally warmed up to about 200 K during the New-Year-Eve/95, and then cooled down and tested again. Strong field emission in the cavity was activated about 17 MV/m (point B). The hot spots are located in different angular position from the previous one in figure 3. The cavity reached 20 MV/m again (Q recovered also) only with a low RF power process. Similar phenomena was observed and explained in [11].

B. Analysis of Thermal Performance

The experimental data obtained with the T-R mapping is consistent with the thermal analysis if we consider the following assumptions: high efficiency of thermometer at high heat flux, heat transfer governed by Kapitza regime, and electron trajectories impacts over a large area.

The magnetic field heating at equators of the 5th cell, for $E_{acc}=11.2$ MV/m and $R_s=30$ n Ω , gives only $\Delta T=5$ mK. From the RF measurement, we can estimate the total dissipated power in the cavity and distinguish the two main contributions: (1) dissipated power in the cavity wall due to magnetic losses: $Pr_f=13$ W, covering entire 9 cells, and (2) the power related to the electron FE: $P_{elec}=173$ W, focusing on local region.

The very high value ΔT measured in this region (100mK-3.3K) can only be explained by assuming that the efficiency of a scanning thermometer increases strongly with the heat flux density at the interface of cavity wall and HeII. This tendency has been observed in several thermometer calibration. We can estimated a heat flux density of 5 W/cm² in the region $\Delta T=3$ K based on experimental values of Kapitza conductance for Nb. Such a high heat flux density is slightly less than the critical heat flux densities reported in experiments with metallic flat heaters in HeII [12], So it is believed that the heat transfer is in the regime governed by Kapitza conductance. The integration of the product of Kapitza conductance and ΔT over the heated region leads to a total heat power going to He bath: $Q\sim 100$ W. This value is consistent with the RF measurements of the experiment.

C. Identifying of FE Origins

Locating origins of FE and TB is very important to understand the influence of various cavity processing and also to a guided reparation of defected cavities. The measured hot spots directly indicate the location of a defect in case of TB. However, the measured hot spots only indicate the landing of impacting FE electrons, but not the emitter.

The simulation of FE electron trajectories demonstrate the following interesting results: FE electrons from an emitter can impact over a very large area, the shape of trajectories are sensitive to emitter location (So), and an emitter responsible

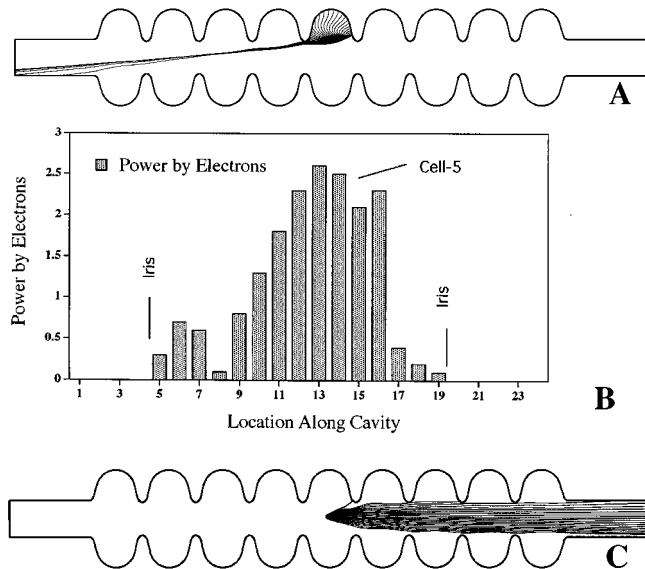


Figure 4: (A) FE electron trajectories of an emitter located at $So=8$ cm. (B) Power distribution contributed by impacting FE electrons from $So=8$ cm. (C) Electron trajectories, $So=9$ cm. for the heating shown in figure 3 is successfully identified.

Since electron trajectories, impacting electron energy and power deposition distribution (dP/ds vs. s) are controlled by the E_{acc} and So , a series of simulations are performed by changing So at $E_{acc}=11.2$ MV/m, assume $\beta=200$, Se (emitter area) = 1×10^{-13} m². It is found that an emitter located at $So=8$ cm (at the iris area in a curvilinear co-ordination) has electron trajectories shown in figure 4A. Its power distribution (dP/ds vs. S) in figure 4B seems to be closed to the shape of the measured temperature distribution. It is indicated that heated area at equator (usually by defects) can also be caused by FE. The β and Se (emitter area) of the candidate emitter were adjusted to fit with the thermal analysis and RF experimental data. For instance, at $E_{acc}=11.2$ MV/m, if $Se=1\times 10^{-13}$ m², $\beta = 400$, the total mean power landed over RF period is 10W.

The FE electron trajectories are very sensitive to the emitter location in the cavity. For example, if an emitter locates at $So=9$ cm, FE electrons are driven out of the initial cell and rush to the cut-off tube of the cavity (Figure 4C).

IV. FUTURE DEVELOPMENT

The improvement of the mechanical system and cabling of the mapping is scheduled in the May of 95. The computer data acquisition for photodiodes will also be commissioned at next test.

V. ACKNOWLEDGEMENT

We sincerely thank P. Kneisel (CEBAF), W. Weingarten (CERN), H. Padamsee, J. Gruber, W. Hartung (Cornell), M. Champion (Fermilab), C. Pagani (INFN), B. Bonin (Saclay) and G. Wueller, R. Roeth (Wuppertal) for many fresh discussions and hints. Sincere thanks are also presented to our DESY colleagues in the cryogenic group, vacuum group, mechanical group, MHF group for their support.

VI. REFERENCES

1. Q. S. Shu et.al., TU-A3-6, CEC/ICMC Conf., Ohio, 1995.
2. T. Junquera et. al. TTP 14, this Conf., PAC/95.
3. D. Proch: Proc. - 5th workshop on RFS, DESY, 1991.
4. R. Sundelin: Proc. - 6th workshop on RFS, CEBAF, 1993
5. H. Padamsee, Applied Supercond. Conf., Boston, 1994.
6. Ph. Bernard et. al., Nucl Inst & Met in Phys Res vol 190
7. Ph. Bernard et. al. & S. Buhler et. al, the 5th (and 6th) workshop on RFS, DESY 1991 (and CEBAF, 1993).
8. Q.S. Shu et..al., IEEE transaction, Vol. 27, No. 2, 1991.
9. Q.S. Shu et.al., Nucl Inst & Met in Phys Res A278. 1989.
10. J. Knobloch, et. al., SRF 94-0419-03, Cornell Univ., 1994
11. B. Bonin et. al., Proc. of 6th workshop on RFS, 1993.
12. M. Fouaidy et al Proc 5th workshop on RFS, DESY,1991.
13. R. Roth and G. Muller et. al., Proc. of the 5th (and 6th) workshop on RFS, DESY 1991 (and CEBAF, 1993).
14. A. Matheisen, D. Trines, TESLA Meeting, 1994.
15. J. Gruber et. al., Nucl Inst & Met in Phy Res A278. 1989.
16. Q. S. Shu et. al., IEEE transaction, Vol. 25, No. 2, 1989.
17. A. Kashani, S. W. Van Sciver, Cryogenics 25, 1985.